

# Subsonic Dynamic Testing of a Subscale ADEPT Entry Vehicle

Juan R. Cruz<sup>1</sup> and Justin S. Green<sup>2</sup>

NASA Langley Research Center, Hampton, Virginia, 23689-2199, USA

The Adaptive Deployable Entry and Placement Technology (ADEPT) is a mechanically-deployed entry system. A sounding rocket test flight of an ADEPT vehicle, known as ADEPT SR-1, was conducted in September 2018. Prior to this sounding rocket test, an investigation was performed using the NASA Langley Research Center 20-ft Vertical Spin Tunnel (VST) to assess the free-flight dynamic characteristics of ADEPT SR-1 at subsonic speeds. The model of ADEPT SR-1 for this VST test was fabricated at 50-percent geometric scale, with dynamically scaled mass properties (Froude scaled) to represent full-scale flight at an altitude of 1.2 km above sea level. The subsonic dynamic characteristics of ADEPT SR-1 were of interest prior to the sounding rocket test because of payload recovery considerations. At low roll rates the model was found to have acceptable dynamic characteristics. It was statically stable in pitch and yaw, exhibiting limit cycle pitch/yaw oscillations of no greater than 20 degrees (the angle between the model's longitudinal axis and nadir). The model was able to recover from large upsets in pitch and yaw, although if sufficiently provoked it tumbled. Damping in roll was low. At high roll rates the pitch and yaw oscillations grew in magnitude and rate. This behavior was also observed during the sounding rocket flight test.

## I. Nomenclature

$C_{D,\text{Eff}}$	= effective drag coefficient
$D$	= reference diameter (from batten tip-to-tip)
$g$	= acceleration of gravity
$I$	= mass moment or product of inertia
$I_{xx}, I_{yy}, I_{zz}$	= mass moments of inertia about the body frame axes and the center of mass
$L$	= length
$m$	= mass
$N$	= scale ratio
$N_g$	= acceleration of gravity scale ratio
$N_I$	= mass moment or product of inertia scale ratio
$N_L$	= length scale ratio
$N_m$	= mass scale ratio
$N_{Re}$	= Reynolds number scale ratio
$N_t$	= time scale ratio
$N_u$	= speed scale ratio
$N_\mu$	= atmospheric coefficient of dynamic viscosity scale ratio
$N_\rho$	= atmospheric density scale ratio
$N_\omega$	= rotation rate scale ratio

---

<sup>1</sup> Aerospace Engineer, Atmospheric Flight and Entry Systems Branch, AIAA Associate Fellow.

<sup>2</sup> Aerospace Engineer, Atmospheric Flight and Entry Systems Branch, AIAA Student Member.

$p, q, r$	= roll, pitch, and yaw rotation rates, respectively, about the body frame axes
$P_{VST}$	= static atmospheric pressure in the VST
$q_{VST}$	= dynamic pressure in the VST
$R$	= gas constant for air (287.054 J/(kg•K))
$Re$	= Reynolds number
$R_x, R_y, R_z$	= Euler angles defining the attitude of the model; rotation sequence $R_x \rightarrow R_y \rightarrow R_z$
$S$	= reference area
$T_{VST}$	= static atmospheric temperature in the VST
$T_{11}, T_{12}, T_{13}$	= elements of a transformation matrix
$t$	= time
$U$	= speed
$V_{\text{Eff}}$	= effective vertical airspeed of the model in the VST
$V_{VST}$	= airspeed in the VST
$X_{VST}, Y_{VST}, Z_{VST}$	= location of the model's nose in the inertial frame
$X_{VST,\text{CoM}}$	= location of the model's center of mass in the inertial frame along the $X_{VST}$ axis
$x, y, z$	= body frame axes
$x_{\text{CoM}}, y_{\text{CoM}}, z_{\text{CoM}}$	= location of the center of mass in the body frame
$\Theta$	= nadir angle
$\theta$	= standard aerospace elevation Euler angle
$\mu$	= atmospheric coefficient of dynamic viscosity
$\rho$	= atmospheric density
$\omega$	= rotation rate
$\omega_{qr}$	= pitch/yaw rotation rate

#### Subscripts

FS	= full-scale
M	= model

#### Abbreviations

ADEPT	= Adaptive Deployable Entry and Placement Technology
AFRC	= Armstrong Flight Research Center
ARC	= Ames Research Center
CoM	= center of mass
FSV	= ADEPT SR-1 full-scale vehicle
LARC	= Langley Research Center
SIDPAC	= System Identification Programs for AirCraft
SR	= Sounding Rocket
VST	= Vertical Spin Tunnel

## II. Introduction

The Adaptive Deployable Entry and Placement Technology (ADEPT) is a mechanically-deployed entry system with a variety of applications [1, 2]. A sounding rocket (SR) test flight of an ADEPT vehicle, shown in Fig. 1 and known as ADEPT SR-1, was conducted in September 2018. Prior to this sounding rocket test, an investigation was performed using the NASA Langley Research Center (LaRC) 20-ft Vertical Spin Tunnel (VST) to assess the free-flight dynamic characteristics of ADEPT SR-1 at subsonic speeds. The model of ADEPT SR-1 for this VST test was fabricated at 50-percent geometric scale, with dynamically scaled mass properties (Froude scaled). The subsonic dynamic characteristics of ADEPT SR-1 were of interest prior to the sounding rocket test because of payload recovery considerations. This paper describes the ADEPT SR-1 model, VST test, and test results.

The NASA Ames Research Center (ARC) led the ADEPT project, with support from NASA LaRC and the NASA Armstrong Flight Research Center (AFRC).

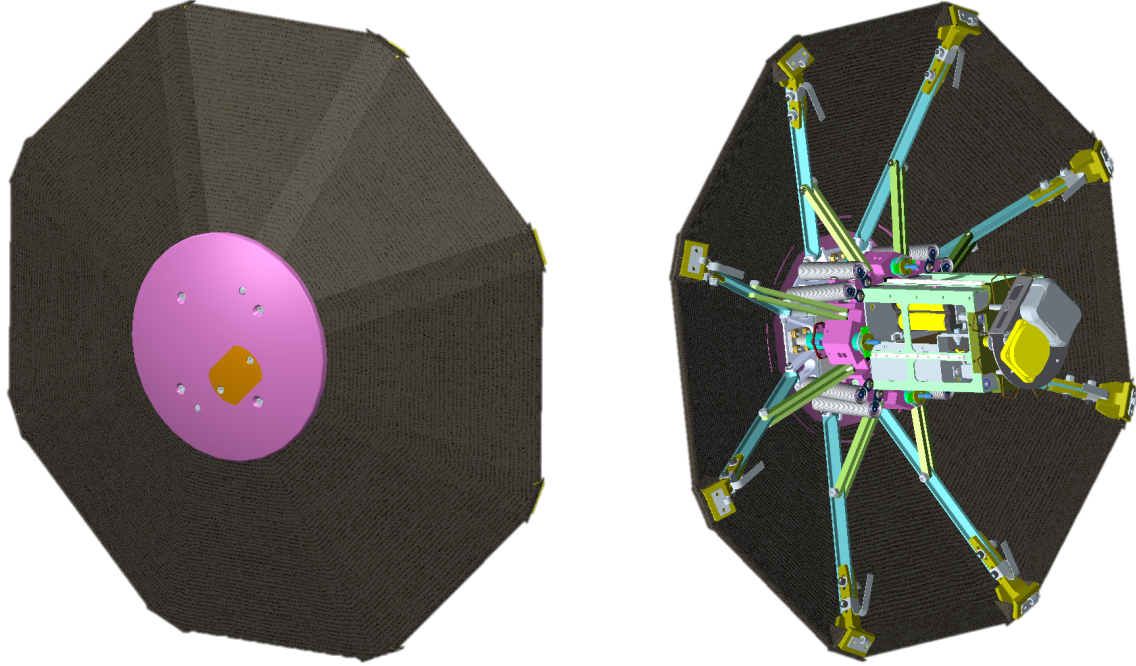


**Fig. 1 ADEPT SR-1 front and rear views. Image credit: NASA ARC.**

### III. Test Goal and Objectives

The goal of the wind tunnel test described herein was to assess the dynamic behavior of ADEPT SR-1 at subsonic speed and the expected landing altitude of 1.2 km above sea level. These goals were achieved by accomplishing the following objectives.

- 1) Obtaining the dynamic characteristics (i.e., attitude and rotation rates versus time).
- 2) Determining the effects of large upsets on the dynamic characteristics (e.g., damping, tumbling).
- 3) Determining the effects of the axial center of mass (CoM) location on the dynamic characteristics.
- 4) Determining the effects of high roll rates on the dynamic characteristics.
- 5) Determining the drag coefficient and full-scale descent rate.

### IV. Model

The model was a 50-percent<sup>†</sup> geometrically-scaled version of ADEPT SR-1 full-scale vehicle (FSV<sup>‡</sup>). The mass properties of the model were dynamically scaled (Froude scaled); thus, the model would simulate the behavior of the FSV. Geometrically and dynamically scaling the model allowed transformation of the test results to their equivalent values for the FSV. A drawing of the FSV is shown in Fig. 2. Photographs of the model are shown in Fig. 3. The model was principally fabricated from plastic by a three-dimensional printer. In addition, the model had a few metal parts (notice, for example, the square metal ballast masses seen in the rear view of Fig. 3). It was possible to easily change the axial CoM of the model by moving a mass inside the chassis (the rectangular cuboid seen in the rear view of Fig. 3). The circular dots seen in the front view of Fig. 3 were reflectors for use by the motion capture system in the VST. The model was painted flat black to avoid undesired reflections that could be picked up by the motion capture system. The body reference frame used in the present paper is shown in Fig. 4; the origin of this reference frame was at the nose for both the model and the FSV.

---

<sup>†</sup> A set of 15-percent geometrically-scaled models were also fabricated. Their mass properties were dynamically scaled to simulate full-scale flight at an altitude of 15 km above sea level. However, their small size precluded accurate measurement of their mass properties, and their location and attitude in the wind tunnel while being tested. The data acquired from these models was of doubtful accuracy. Thus, they are not discussed further in this paper.

<sup>‡</sup> From this point on, the ADEPT SR-1 full-scale vehicle will be referred to by the abbreviation FSV.

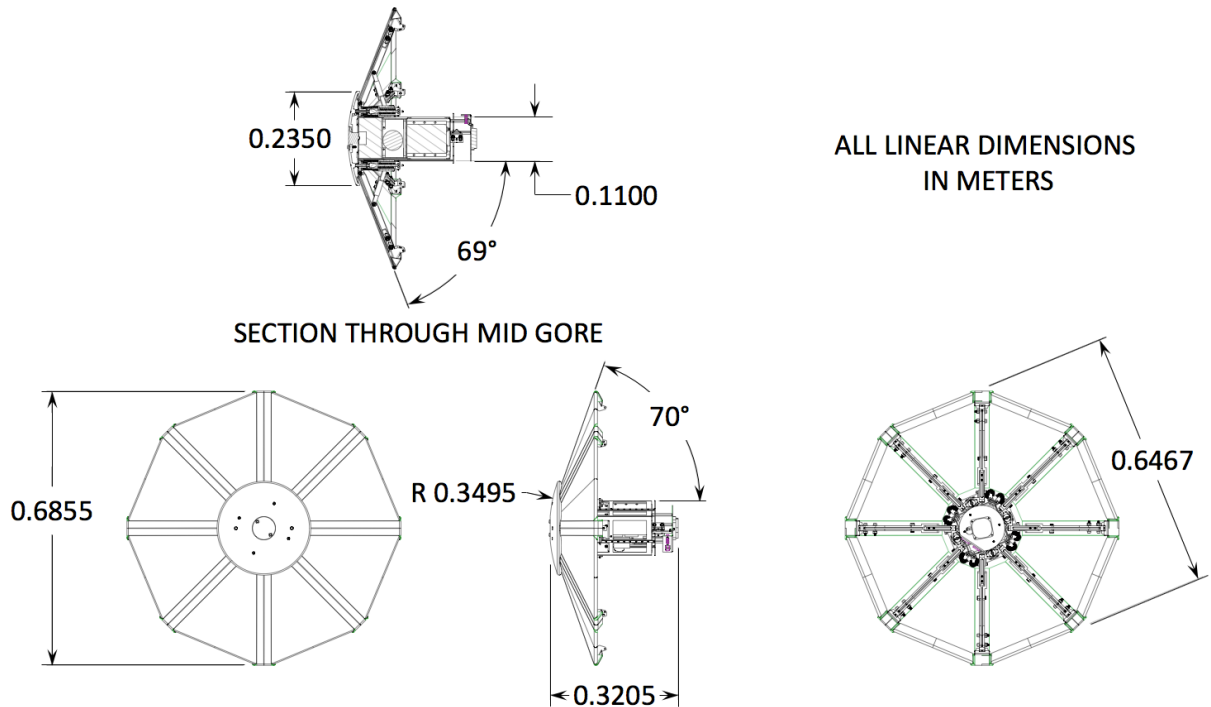


**Fig. 2.** Drawing of the full-scale ADEPT SR-1. Original image credit: C. Kruger, NASA ARC.

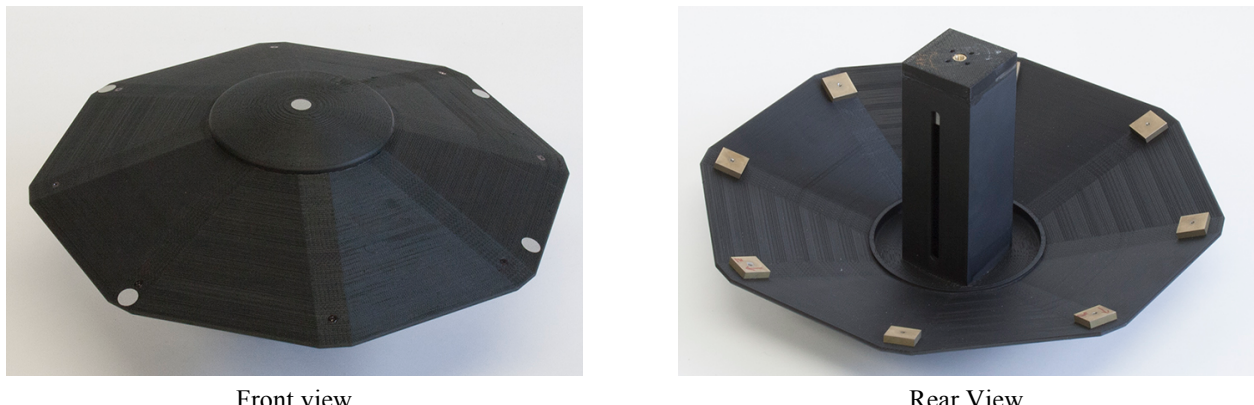


**Fig. 3.** Wind tunnel model.

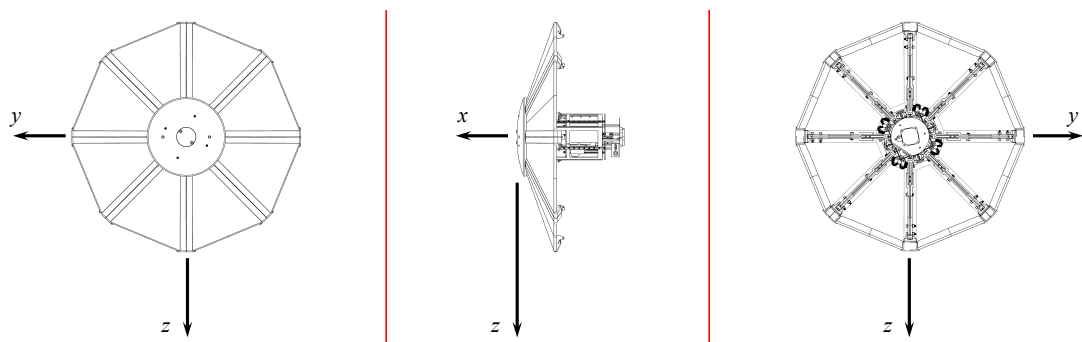


**Fig. 4.** Body reference frame. Original image credit: C. Kruger, NASA ARC.

The dynamic scaling of the model was specified by a set of scaling ratios,  $N$ , defined as

$$N = \frac{\text{model parameter}}{\text{full-scale parameter}} \quad (1)$$

The scaling ratios of interest are defined in Table 1. The subscripts “M” and “FS” indicate whether the value is for the model or the FSV, respectively. For test planning purposes the values used for  $g_M$ ,  $\rho_M$ , and  $\mu_M$  were those at sea level [3]. This was appropriate since the VST is located at sea level. (Analyses of the test results used the measured values of  $\rho_M$  and  $\mu_M$  as discussed later in this paper.) For the FSV the values of  $g_{FS}$ ,  $\rho_{FS}$ , and  $\mu_{FS}$  used were for an altitude of 1.2 km [3]. In general, it is desirable to match the FSV Reynolds number on the model; in other words, it is desirable to have  $N_{Re} = 1$ . Note, however, that the model Reynolds number did not match that for the FSV:  $N_{Re} = 0.389$ . Because the aerodynamic forces and moments on both the FSV and the model are dominated by surface pressures that are principally defined by separated flow, the lack of match in Reynolds number between the FSV and model was considered to have a minimal effect on the results.

The scaling ratios in Table 1 were used to specify the model “As-designed” dimensions and mass properties. The dimensions and mass properties of both the FSV and model are shown in Table 2. For the models in Table 2 both the “As-designed” and “As-built” values are given. The “As-built” mass properties of the models were close to the desired “As-designed” values. Note that the principal difference between the “As-built Nominal CoM” and “As-built Forward CoM” models was their axial CoM location. This difference was intentional in order to pursue test objective 3.

**Table 1. Scaling ratios definitions and values.**

Scaling Ratio	Equation	Value	Remarks
Acceleration of gravity, $N_g$	$N_g = g_M/g_{FS}$	1.0004	$g_M = 9.80665 \text{ m/s}^2$ $g_{FS} = 9.8029 \text{ m/s}^2$
Atmospheric density, $N_\rho$	$N_\rho = \rho_M/\rho_{FS}$	1.124	$\rho_M = 1.225 \text{ kg/m}^3$ $\rho_{FS} = 1.090 \text{ kg/m}^3$
Atmospheric coefficient of dynamic viscosity, $N_\mu$	$N_\mu = \mu_M/\mu_{FS}$	1.022	$\mu_M = 1.7894 \cdot 10^{-5} \text{ N}\cdot\text{s/m}^2$ $\mu_{FS} = 1.7515 \cdot 10^{-5} \text{ N}\cdot\text{s/m}^2$
Length, $N_L$	$N_L = L_M/L_{FS}$	0.500	50-percent scale
Mass, $N_m$	$N_m = m_M/m_{FS} = N_\rho N_L^3$	0.1405	
Mass moments and products of inertia, $N_I$	$N_I = I_M/I_{FS} = N_\rho N_L^5$	0.0351	
Time, $N_t$	$N_t = t_M/t_{FS} = \sqrt{N_L/N_g}$	0.7070	
Speed, $N_U$	$N_U = U_M/U_{FS} = \sqrt{N_g N_L}$	0.7072	
Rotation rate, $N_\omega$	$N_\omega = \omega_M/\omega_{FS} = \sqrt{N_g/N_L}$	1.414	Model rotates faster than the FSV.
Reynolds number, $N_{Re}$	$N_{Re} = Re_M/Re_{FS} = (N_\rho/N_\mu) \sqrt{N_g N_L^3}$	0.389	Reynolds number is not matched.

**Table 2. Full-scale and model dimensions and mass properties.**

	<b>Full-scale</b>	<b>Model As-designed</b>	<b>Model As-built Nominal CoM</b>	<b>Model As-built Forward CoM</b>
Scale	100 percent	50 percent	50 percent	50 percent
Maximum diameter (reference length), $D$ (m)	0.700	0.350	0.350	0.350
Reference area $(\pi D^2/4)$ , $S$ ( $\text{m}^2$ )	0.3849	0.09621	0.09621	0.09621
Center of mass location, $[x_{\text{CoM}}, y_{\text{CoM}}, z_{\text{CoM}}]$ (mm)	[-109.80, 0.25, 0.25]	[-54.90, 0.13, 0.13]	[-54.89, 0.48, 0.66]	[-37.90, 0.38, 0.66]
Dimensionless axial center of mass location, $x_{\text{CoM}}/D$	-0.157	-0.157	-0.157	-0.108
Mass, $m$ (kg)	8.490	1.193	1.226	1.226
Mass moment of inertia, $I_{xx}$ ( $\text{kg}\cdot\text{m}^2$ )	0.2500	$8.780\cdot 10^{-3}$	$10.60\cdot 10^{-3}$	$10.61\cdot 10^{-3}$
Mass moment of inertia, $I_{yy}$ ( $\text{kg}\cdot\text{m}^2$ )	0.1722	$6.048\cdot 10^{-3}$	$6.066\cdot 10^{-3}$	$6.670\cdot 10^{-3}$
Mass moment of inertia, $I_{zz}$ ( $\text{kg}\cdot\text{m}^2$ )	0.1719	$6.037\cdot 10^{-3}$	$6.154\cdot 10^{-3}$	$6.760\cdot 10^{-3}$

Notes:

- 1) The FSV maximum diameter in this table,  $D=0.700$  m, is different from the value shown in Fig. 2, 0.6855 m. The reason for this difference is in the tolerance for fabrication and deployment of the FSV. The nominal value of  $D$  is 0.700 m, but it has a tolerance of 0.71 m Max and 0.68 m Min. Part of the reason for this diameter variation is the related variation in the rib angle ( $70^\circ$  as shown in Fig. 2), which has a tolerance of several degrees. All these variations are associated with the fact that ADEPT SR-1 is a textile deployable structure.
- 2) The FSV mass properties were the estimated values as of October 12, 2016, and are the values used in this paper. The sounding rocket test flight mass of ADEPT SR-1 was 11.013 kg.
- 3) The mass moments of inertia are about the CoM.

## V. Test Facility

Testing was conducted at the NASA LaRC 20-Foot Vertical Spin Tunnel. The VST is shown in cross-section (left drawing) and in operation (right photograph) in Fig. 4. This wind tunnel provides vertical flow for free-flight simulations in a gravity field. Horizontally the test section is a 12-sided polygon, 6.1 m across the flats. Vertically the test section is 7.6 m high. Windows around the periphery of the test section allows viewing the model in flight. The maximum operating airspeed and dynamic pressure of the VST are 26 m/s and 411 Pa, respectively at sea level conditions. Airspeed in the VST is controlled by an operator who can vary it rapidly to maintain the vertical position of the model. A motion-capture system allows for the recording of the model position and attitude, concurrent with the VST operating parameters (e.g., dynamic pressure). A model swing rig (Space Electronics Model KSR330-6) in a laboratory adjacent to the VST allows for the accurate measurement of the model mass properties (i.e., mass, center of gravity, and mass moments of inertia).

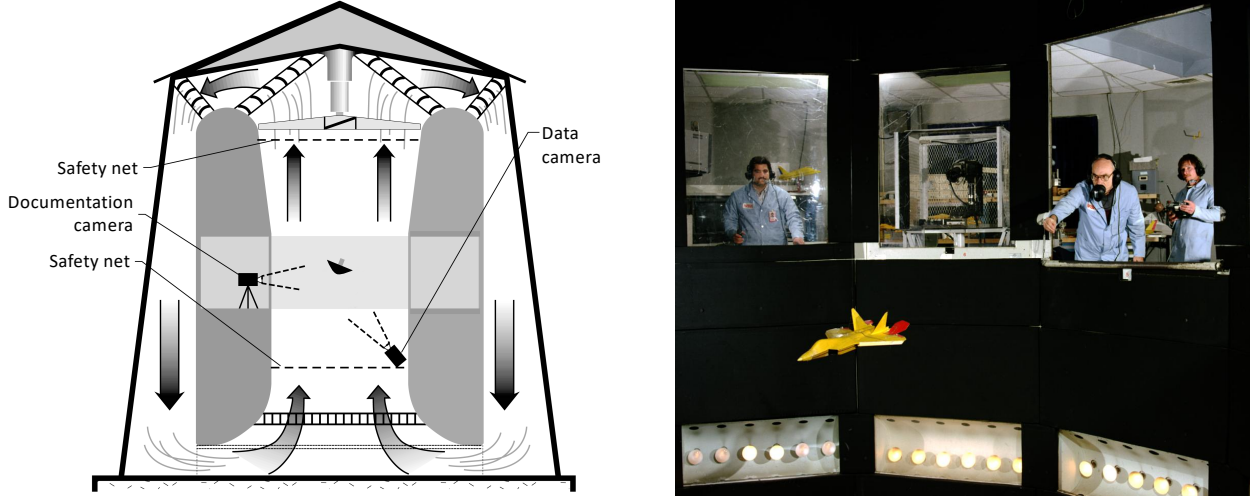


**Fig. 4** Vertical Spin Tunnel: cross-section and test section photograph. Drawing and photo credit: NASA LaRC.

## VI. Test Procedures and Data Acquisition

Three test procedures were used. These were *unperturbed*, *perturbed*, and *high roll rate*.

- 1) *Unperturbed tests*. The model was placed in the airstream by a technician, while the operator adjusted the wind tunnel speed to make the model “float.” The model was then released while aligned with the wind tunnel flow (i.e., vertically), and with minimal roll, pitch, and yaw rotation rates. These tests resulted in model limit cycle pitch/yaw oscillations.
- 2) *Perturbed tests*. The model was placed in the airstream in the same manner as with the unperturbed tests. Once the model was released and established in the airflow, a technician reached out to the model with a pole and perturbed the model in attitude and rotation rates. On some attempts the model would return to limit cycle pitch/yaw oscillations, while on other attempts the model would tumble.
- 3) *High roll rate tests*. The operator adjusted the wind tunnel speed to make the model “float.” Then, he model was inserted in the airstream by a technician at an intentionally high roll rate, while aligned with the wind tunnel flow, and with minimal pitch/yaw rotation rates. These tests resulted in model limit cycle pitch/yaw oscillations, albeit larger than for the unperturbed tests with low roll rates.

For all test procedures the specific run (i.e., a continuous test interval) was terminated when the model touched the walls or nets of the VST.

Video of the model in flight was recorded during testing. In addition, the following data were acquired at a sampling rate of 150 Hz.

- Static atmospheric pressure,  $p_{\text{VST}}$  .
- Static atmospheric temperature,  $T_{\text{VST}}$  .
- Dynamic pressure,  $q_{\text{VST}}$  .
- Position of the model nose in the VST frame,  $(X_{\text{VST}}, Y_{\text{VST}}, Z_{\text{VST}})$  . The VST frame is an inertial frame with origin within the test section. The  $X_{\text{VST}}$  axis points down. The  $Y_{\text{VST}}$  and  $Z_{\text{VST}}$  lie in the horizontal plane; they are perpendicular to the  $X_{\text{VST}}$  axis and to each other.
- Euler angles,  $(R_x, R_y, R_z)$  , defining the model attitude with respect to the VST frame. The rotation sequence of these Euler angles was  $R_x \rightarrow R_y \rightarrow R_z$  . Note that these are not the usual aerospace Euler angles – the rotation sequence is different. This choice of Euler angles was required to avoid the singularity with the usual aerospace Euler angle  $\theta$  (elevation) when  $\theta = \pm \pi/2$  .
- Time,  $t_M$  .

These quantities were denoted as “source data.” All other quantities were denoted “derived quantities” since they were calculated from the source data.

## VII. Data Analyses

The first step in the data analyses was to smooth the source data to remove noise and allow for accurate differentiation of the data with respect to time. Smoothing was performed using the global smoothing in the frequency domain approach described in Reference [4], section 11.2.3. A modified version of the System Identification Programs for AirCraft (SIDPAC) software (Ref. [4], chapter 12) was used to perform the smoothing. In this smoothing procedure each quantity in the source data are fitted by a finite Fourier series. Higher Fourier coefficients, associated with noise, are discarded. The truncated Fourier series then represents a specific quantity. This truncated Fourier series can be analytically differentiated to yield derivatives that are internally consistent.

From the smoothed source data numerous quantities of interest were calculated using well-known flight mechanics relationships. Conversion of model quantities to FSV quantities were performed as necessary using the appropriate scaling ratios described previously. The quantities of interest discussed herein are the following.

- Nadir angle:  $\Theta$ . This is the angle between the model's longitudinal axis,  $x$ , and the  $X_{\text{VST}}$  axis (nadir).

The nadir angle was calculated from the equation

$$\Theta = \arccos[\cos(R_y)\cos(R_z)] \quad 0 \leq \Theta \leq \pi \quad (2)$$

If the model was pointing straight down,  $\Theta = 0$ . Note that  $\Theta$  is always greater than or equal to zero.

Also, note that  $\Theta$ ,  $R_y$ ,  $R_z$  have the same value for both the model and FSV (they are dimensionless quantities); thus, they did not need to be scaled from the model to the FSV. The nadir angle was used as a metric to evaluate the dynamic behavior of the model (e.g., impact angle at landing, propensity of the model to tumbling due to a perturbation in pitch and/or yaw).

- Full-scale vehicle roll, pitch, and yaw rotation rates about its body axes:  $p_{\text{FS}}$ ,  $q_{\text{FS}}$ , and  $r_{\text{FS}}$ , respectively. These rates were calculated from the equations

$$\begin{Bmatrix} p_{\text{FS}} \\ q_{\text{FS}} \\ r_{\text{FS}} \end{Bmatrix} = \frac{1}{N_{\omega}} \begin{bmatrix} \cos R_y \cos R_z & \sin R_z & 0 \\ -\cos R_y \sin R_z & \cos R_z & 0 \\ \sin R_y & 0 & 1 \end{bmatrix} \begin{Bmatrix} \dot{R}_x \\ \dot{R}_y \\ \dot{R}_z \end{Bmatrix} \quad (3)$$

Note that the time derivatives for  $R_x$ ,  $R_y$ , and  $R_z$  were with respect to model test time,  $t_M$ , as recorded during the test; the conversion of the rotation rates from the model to the FSV was accomplished by the scaling ratio  $1/N_{\omega}$ .

- Full-scale vehicle pitch and yaw rotation rate:  $\omega_{qr,\text{FS}}$ . This quantity was used to evaluate the combination of pitch and yaw rates. It was calculated from the equation

$$\omega_{qr,\text{FS}} = \sqrt{q_{\text{FS}}^2 + r_{\text{FS}}^2} \quad (4)$$

Note that  $\omega_{qr,\text{FS}}$  is always greater than or equal to zero. This quantity was used as a metric to evaluate the dynamic behavior of the model.

- Effective drag coefficient:  $C_{D,\text{Eff}}$ . This was an average drag coefficient based on the descent rate of the model. It was calculated from the equation

$$C_{D,\text{Eff}} = \frac{2m_M(g_M - \ddot{X}_{\text{VST,CoM}})}{\rho_M V_{\text{Eff}}^2 S_M} \quad (5)$$

where  $\ddot{X}_{\text{VST,CoM}}$  is the vertical acceleration of the model's center of mass in the VST frame (inertial frame),  $\rho_M$  is the atmospheric density in the VST, and  $V_{\text{Eff}}$  is the effective vertical airspeed of the

model in the VST. Equations used for the calculation of  $\dot{X}_{\text{VST,CoM}}$ ,  $\rho_M$ , and  $V_{\text{Eff}}$  are presented in the appendix. Note that  $C_{D,\text{Eff}}$  is dimensionless; thus, it can be calculated using values from the model, and is valid for the model and the FSV.

## VIII. Results and Observations

The results presented herein are organized by test procedure: unperturbed, and high roll rate.

### A. Unperturbed Tests

Example time histories of  $p_{\text{FS}}$ ,  $\Theta$ , and  $\omega_{qr,\text{FS}}$  for a specific unperturbed run are shown in Fig. 5 (nominal CoM location). The parameters of interest for the unperturbed runs were the statistics of  $\Theta$ ,  $\omega_{qr,\text{FS}}$ , and  $C_{D,\text{Eff}}$ . For these runs both the nominal and forward positions of the CoM were used. Results for the nominal CoM location were obtained from 10 runs consisting of 35976 data points (total) and representing approximately 339 s of full-scale flight. The range of roll rates,  $p_{\text{FS}}$ , for these data were from -12.9 to 13.0 deg/s. Results for the forward CoM location were obtained from 6 runs consisting of 20941 data points (total) and representing approximately 197 s of full-scale flight. The range of roll rates,  $p_{\text{FS}}$ , for these data were from -12.7 to 13.5 deg/s. The unperturbed runs statistics for  $\Theta$  and  $\omega_{qr,\text{FS}}$  are presented in Table 3. From the results in this table it can be observed that it is unlikely that  $\Theta$  will exceed 19.2 deg, and that  $\omega_{qr,\text{FS}}$  will exceed 120.3 deg/s for the nominal CoM location (assuming no turbulence in the atmosphere). The corresponding values of  $\Theta$  and  $\omega_{qr,\text{FS}}$  for the forward CoM location are somewhat smaller: 15.3 deg and 99.1 deg/s, respectively.

**Table 3. Unperturbed runs statistics for  $\Theta$  and  $\omega_{qr,\text{FS}}$ .**

	$\Theta$ (deg)		$\omega_{qr,\text{FS}}$ (deg/s)	
	Nominal CoM	Forward CoM	Nominal CoM	Forward CoM
Maximum	19.2	15.3	120.3	99.1
99.5 percentile	16.4	14.0	106.2	90.3
97.5 percentile	14.4	12.0	93.7	77.2
90.0 percentile	12.1	10.1	78.6	64.5
75.0 percentile	10.1	8.2	65.8	52.6
Median	7.8	6.1	50.9	40.2
Mean	7.8	6.3	50.6	40.6

The mean values of  $C_{D,\text{Eff}}$  for the nominal and forward CoM locations were 0.967 and 0.933, respectively. They were calculated from the same sets of data points as  $\Theta$  and  $\omega_{qr,\text{FS}}$  described above. There was a -3.5 percent difference in the values of  $C_{D,\text{Eff}}$  between the forward and nominal CoM locations. The corresponding FSV descent rates at an altitude of 1.2 km (using the values of  $C_{D,\text{Eff}}$  just cited, the values of  $g_{\text{FS}}$  and  $\rho_{\text{FS}}$  from Table 1, and the values of  $m_{\text{FS}}$  and  $S_{\text{FS}}$  from Table 2) were 20.3 and 20.6 m/s for the nominal and forward CoM locations, respectively.<sup>§</sup> The absolute values of  $C_{D,\text{Eff}}$  and descent rates should be regarded with caution, as an estimate for the uncertainty of  $V_{\text{Eff}}$  (the principal contributor to the uncertainty in  $C_{D,\text{Eff}}$ ) was not available (see Eq. (5) for the relationship between  $V_{\text{Eff}}$  and  $C_{D,\text{Eff}}$ ).

<sup>§</sup> Using the actual mass of ADEPT SR-1 as flown during the sounding rocket test (11.013 kg, see Note 2 of Table 2), yields terminal descent rates of 23.1 and 23.5 m/s for the nominal and forward CoM locations, respectively.

The following qualitative observations were made during unperturbed testing.

- 1) With the CoM at its nominal location ( $x/D = -0.157$ ), the model was statically and stable and exhibited limit cycle pitch/yaw oscillations of relatively small amplitude (less than 20 deg, see Table 3).
- 2) With the CoM at its forward location ( $x/D = -0.108$ ), the model was statically and stable and exhibited limit cycle pitch/yaw oscillations of relatively small amplitude (less than 16 deg, smaller than those for the nominal CoM location, see Table 3).
- 3) The model does not have an observable tendency to autorotate in roll (see, for example, the time history of  $p_{FS}$  in Fig. 5).
- 4) Roll damping was low (see, for example, the time history of  $p_{FS}$  in Fig. 5).

## B. Perturbed Tests

During perturbed tests the model was intentionally upset to find its tumbling threshold. Although an exact tumbling perturbation could not be identified, perturbances that did not result in tumbling yielded information on the dynamic stability limits of the model. An example of a perturbed run is shown in Fig. 6 (forward CoM location). The perturbation occurs at approximately 4.2 s. The roll rate increases from approximately 0 to 35 deg/s. Both  $\Theta$  and  $\omega_{qr,FS}$  increased to values much higher than those observed during the unperturbed runs (compare values in Fig. 6 to those shown in Table 3), but damped out over the next 18 s. Table 4 shows the highest values of  $\Theta$  and  $\omega_{qr,FS}$  observed during testing for runs in which the model recovered from the initial perturbation and did not tumble. Because specific values of  $\Theta$  and  $\omega_{qr,FS}$  could not be targeted, it is possible that the model is even more resistant to tumbling than indicated by the results in Table 4.

**Table 4. Results of perturbed runs for which tumbling did not occur.**

$(\Theta)_{Max}$ (deg)		$(\omega_{qr,FS})_{Max}$ (deg/s)	
Nominal CoM	Forward CoM	Nominal CoM	Forward CoM
57.8	40.8	539	370

The following qualitative observations were made during perturbed testing.

- 1) The model was able to recover from large perturbations in pitch/yaw without tumbling for both center of mass locations. However, it took many oscillations to return to its limit cycle oscillation behavior (see Fig. 6).
- 2) Once the model tumbled, it started rotating rapidly in pitch/yaw. There was no indication that the model would regain limit cycle oscillation flight once it tumbled.
- 3) Once the model tumbled it tended to glide (i.e., move sideways).

## C. High Roll Rate Tests

Several runs were conducted at high roll rates (i.e., large values of  $|p_{FS}|$ ) to assess its effect on the dynamics of the model. Typical results are shown in Fig. 7 (nominal CoM location). The roll rate was high, with values of  $|p_{FS}|$  between 190 and 250 deg/s. Over the first 12 s both  $\Theta$  and  $\omega_{pr,FS}$  increased;  $\Theta$  to the approximate range of 21-27 deg, and  $\omega_{pr,FS}$  to the approximate range of 90-130 deg/s. Comparing these interval values with the corresponding columns in Table 3 indicates that the higher roll rate yields significantly higher values of both  $\Theta$  and  $\omega_{pr,FS}$  than those expected for low values of the roll rate ( $|p_{FS}| \leq 13$  deg/s). Also note that the roll damping was low. Over 23 s, the roll rate decreased by about 48 deg/s – a rotational deceleration rate of approximately 2.1 deg/s<sup>2</sup>.

During the ADEPT SR-1 flight test [5], the FSV started spinning in roll early in the flight, at a Mach number of 3.00. The roll rate peaked at 373 deg/s and a Mach number of 0.52 (prior to tumbling). Concurrently with the high roll rate, the pitch/yaw oscillations also increased. At subsonic speeds the pitch/yaw rates and angles were sufficiently high to induce tumbling at a Mach number of 0.26 when the rotation rate was 321 deg/s. The auto-rotating tendency in roll observed during the flight test was not observed during the VST test. However, the link between high roll rate and high pitch/yaw rates was observed during the VST test as described here.

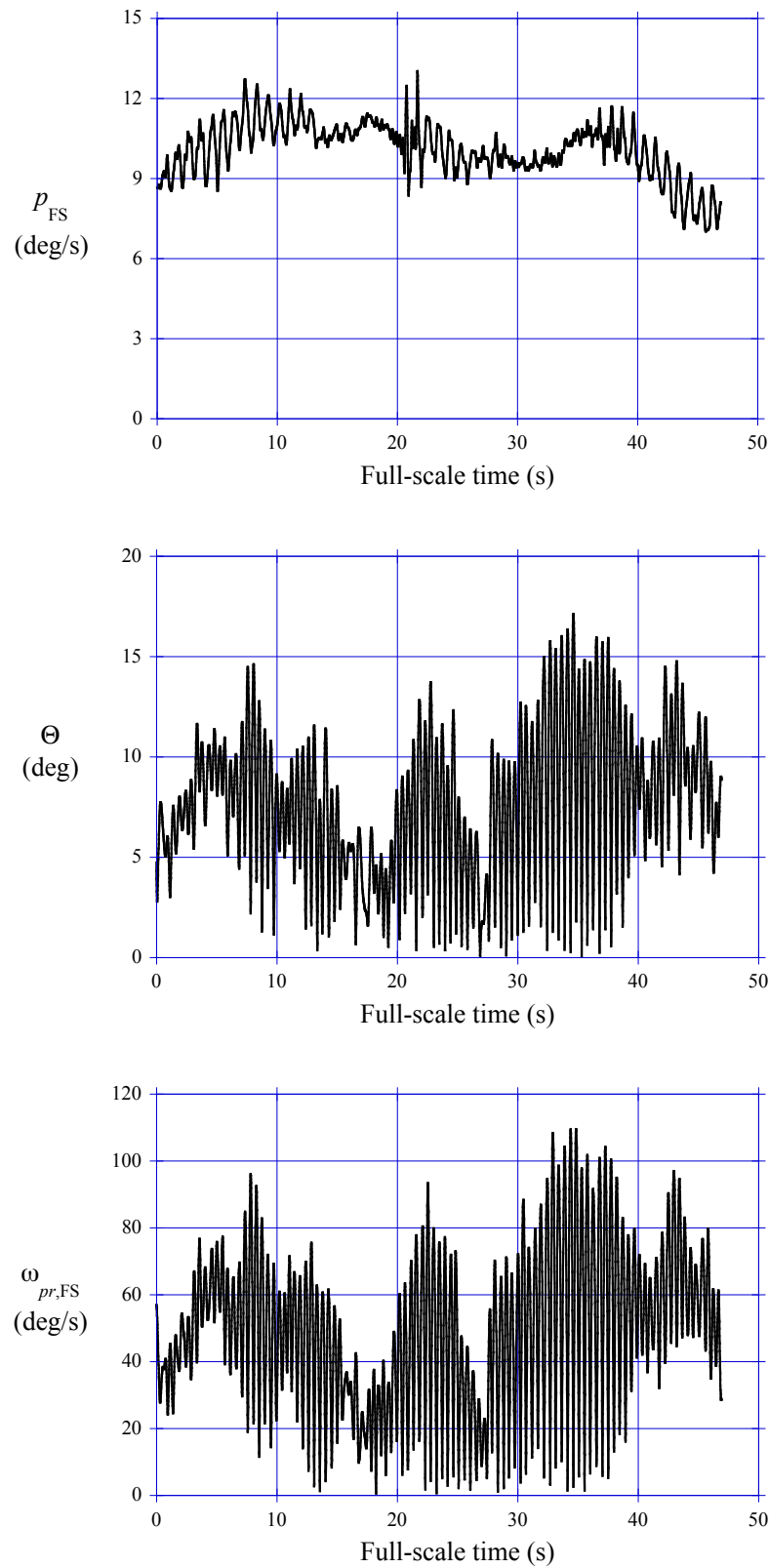


**Fig. 5. Unperturbed dynamics of the model ( $p_{FS}$ ,  $\omega_{pr,M}$ , and time are scaled to the FSV values).**

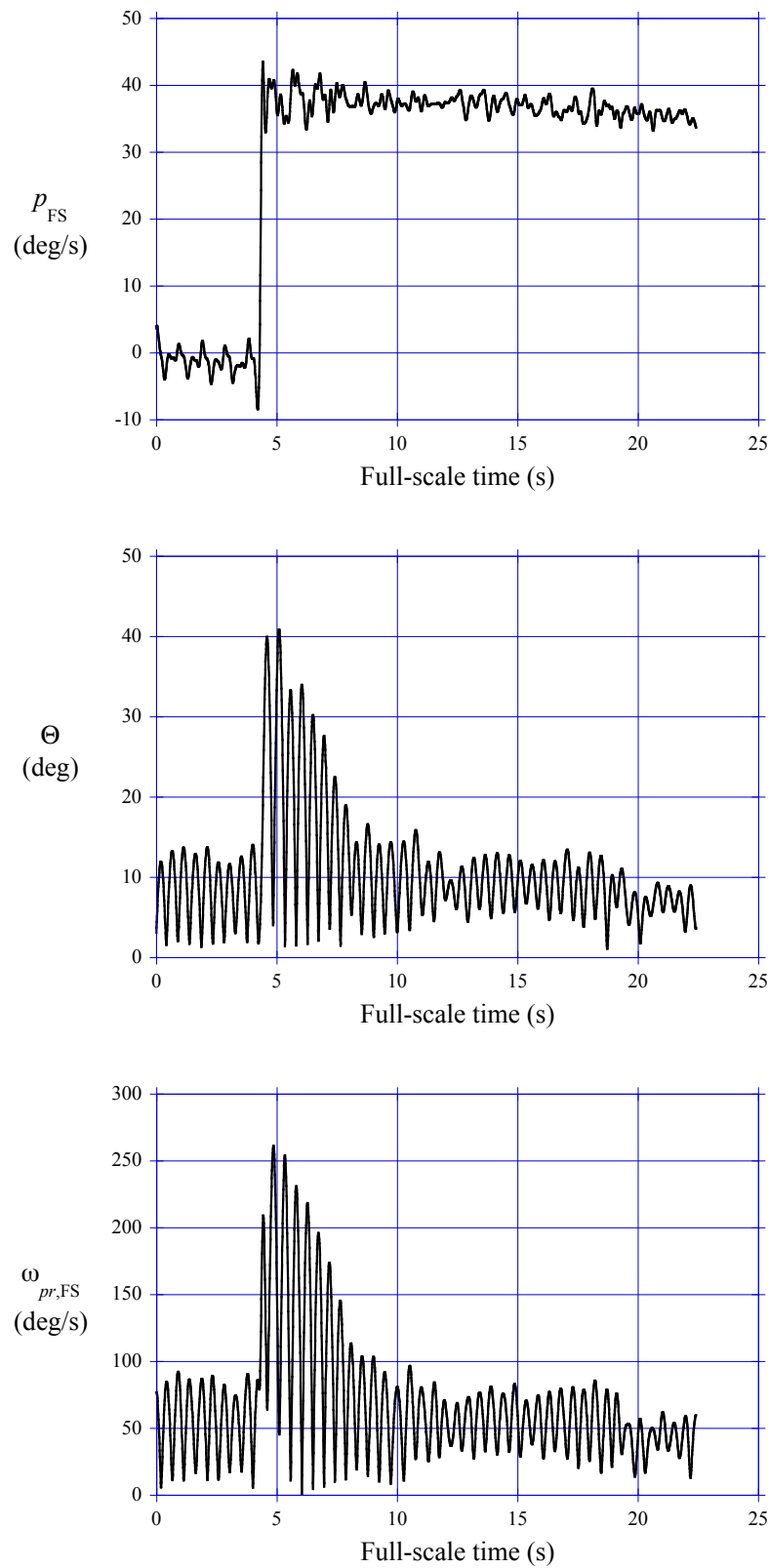


**Fig. 6. Effect of perturbation on the dynamics of the model ( $p_{\text{FS}}$ ,  $\omega_{\text{pr,M}}$ , and time are scaled to the FSV values).**

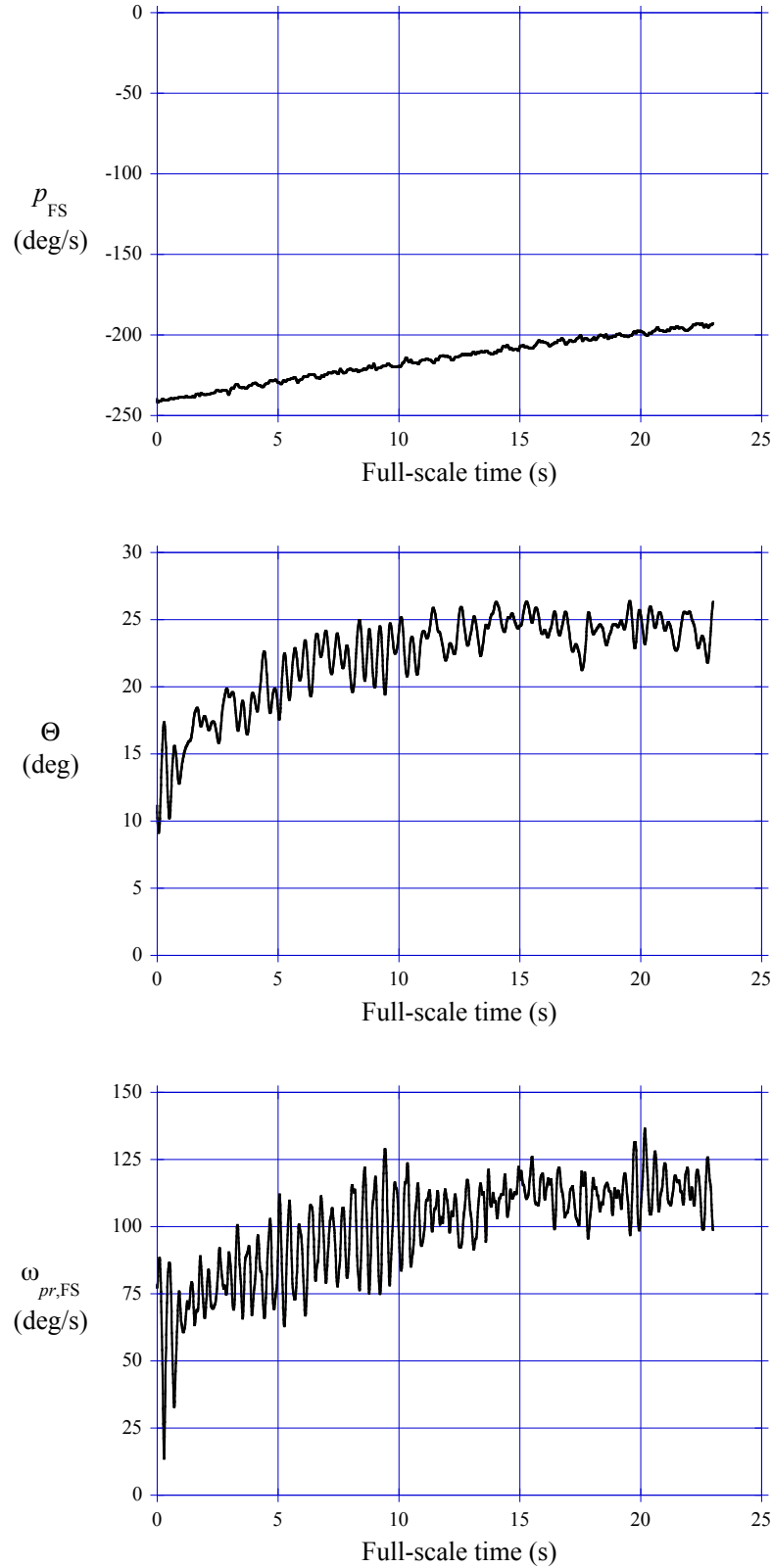


**Fig. 7. Effect of high roll rates on the dynamics of the model ( $p_{FS}$ ,  $\omega_{pr,M}$ , and time are scaled to the FSV values).**

## IX. Concluding Remarks

The dynamic flight characteristics of the FSV at subsonic speeds were investigated by a dynamically-scaled free-flight test. At low roll rates the model was found to have acceptable dynamic characteristics. It was statically stable in pitch and yaw, and exhibited limit cycle pitch/yaw oscillations. The model was able to recover from large upsets in pitch and yaw, although if sufficiently provoked it tumbled. Damping in roll was low. At high roll rates the pitch and yaw oscillations grew in magnitude and rate. This behavior was also observed during the ADEPT SR-1 flight test.

## Acknowledgement

This work was conducted with extensive help from the ADEPT team. The models were fabricated at NASA ARC. Testing was conducted by the staff at the Flight Dynamics Branch at NASA LaRC. The contributions of all individuals involved in the present work are gratefully acknowledged.

## References

- [1] Smith, B., Cassell, A., and Venkatapathy, E., "ADEPT for Secondary Payloads," Presented at the 11<sup>th</sup> International Planetary Probe Workshop, Pasadena, CA, June 16-20, 2014.
- [2] Venkatapathy, E., Wercinski, P., Cassell, A., Smith, B., and Yount, B., "ADEPT – A Mechanically Deployable Entry System Technology in Development at NASA," Presented at the ESA-ESTEC 8<sup>th</sup> European Workshop on TPS and Hot-Structures, Noordwijk, The Netherlands, April 18, 2016.
- [3] Anon., "U.S. Standard Atmosphere, 1976," NOAA, NASA, USAF, NASA-TM-X-74335, October 1976.
- [4] Klein, V. and Morelli, E. A., *Aircraft System Identification – Theory and Practice*, AIAA, Renton, VA, 2006.
- [5] Dutta, S. and Green, J., "Flight Mechanics Modeling and Post Flight Analysis of ADEPT-SR1," to be presented at the 2019 AIAA Aviation Forum.

## Appendix: Additional Equations Needed for the Calculation of the Effective Drag Coefficient

The atmospheric density in the VST was calculated using the equation of state

$$\rho_M = \frac{P_{VST}}{RT_{VST}} \quad (A1)$$

where  $R$  is the gas constant for air (287.054 J/(kg•K)). The effective vertical airspeed,  $V_{Eff}$ , was calculated using the equation

$$V_{Eff} = V_{VST} + \dot{X}_{VST,CoM} \quad (A2)$$

The VST airspeed,  $V_{VST}$ , was calculated using the equation

$$V_{VST} = \sqrt{\frac{2q_{VST}}{\rho_M}} \quad (A3)$$

The quantity  $\dot{X}_{VST,CoM}$  is the vertical velocity of the model's center of mass in the VST frame (inertial frame). It was calculated using the equation

$$\dot{X}_{VST,CoM} = \dot{X}_{VST} + \dot{T}_{11}x_{CoM} + \dot{T}_{12}y_{CoM} + \dot{T}_{13}z_{CoM} \quad (A4)$$

The quantities  $\dot{T}_{11}$ ,  $\dot{T}_{12}$ , and  $\dot{T}_{13}$  are elements of a transformation matrix. They were calculated from the equations

$$\begin{Bmatrix} \dot{T}_{11} \\ \dot{T}_{12} \\ \dot{T}_{13} \end{Bmatrix} = \begin{bmatrix} -\sin R_y \cos R_z & -\cos R_y \sin R_z \\ \sin R_y \sin R_z & -\cos R_y \sin R_z \\ \cos R_y & 0 \end{bmatrix} \begin{Bmatrix} \dot{R}_y \\ \dot{R}_z \end{Bmatrix} \quad (\text{A5})$$

The quantity  $\ddot{X}_{\text{VST,CoM}}$  is the vertical acceleration of the model's center of mass in the VST frame (inertial frame). It was calculated using the equation

$$\ddot{X}_{\text{VST,CoM}} = \ddot{X}_{\text{VST}} + \ddot{T}_{11}x_{\text{CoM}} + \ddot{T}_{12}y_{\text{CoM}} + \ddot{T}_{13}z_{\text{CoM}} \quad (\text{A6})$$

The quantities  $\ddot{T}_{11}$ ,  $\ddot{T}_{12}$ , and  $\ddot{T}_{13}$  are elements of a transformation matrix. They were calculated from the equations

$$\begin{aligned} \ddot{T}_{11} = & -\dot{R}_z(\dot{R}_z \cos R_y \cos R_z - \dot{R}_y \sin R_y \sin R_z) - \dot{R}_z(\cos R_y \sin R_z) \\ & - \dot{R}_y(-\dot{R}_z \sin R_y \sin R_z + \dot{R}_y \cos R_y \cos R_z) - \dot{R}_y(\sin R_y \cos R_z) \end{aligned} \quad (\text{A7})$$

$$\begin{aligned} \ddot{T}_{12} = & -\dot{R}_z(-\dot{R}_z \cos R_y \sin R_z - \dot{R}_y \sin R_y \cos R_z) - \dot{R}_z(\cos R_y \cos R_z) \\ & + \dot{R}_y(\dot{R}_z \sin R_y \cos R_z + \dot{R}_y \cos R_y \sin R_z) + \dot{R}_y(\sin R_y \sin R_z) \end{aligned} \quad (\text{A8})$$

$$\ddot{T}_{13} = -\dot{R}_y^2 \sin R_y + \dot{R}_y \cos R_y \quad (\text{A9})$$